

## Markov-type Evolution of Materials into a Polar State

Jürg Hulliger\*[a]

*Dedicated to Dr. Dr. Herbert Athenstaedt and Prof. Dr. Eiichi Fukada, pioneers in research on the polarity of connective tissues*

**Abstract:** Assembling polar building blocks into a solid material by a Markov-chain process of unidirectional growth principally results in a metastable state that shows effects of macroscopic polarity. Stochastic polarity formation can be described by probabilities for the attachment of building blocks to a surface. Because of the polar symmetry of the building blocks, there is a fundamental difference in the probabilities for attaching them “tip-first” or “back-first” to growth sites at a surface. A difference in the corresponding probabilities drives the evolution of a vectorial property through a gain in configurational entropy. Examples from the mechanical, the crystalline and the biological world demonstrate growth-induced macroscopic polarity. In crystals, growth upon centrosymmetric seeds can produce twinned crystals with a “sectorwise” pyroelectric effect. Polarity formation in connective tissues is explained by a Markov-chain mechanism, which drives the self-assembly of collagen fibril segments. A unified stochastic growth model brings up a general concept for the formation of materials with polar properties.

**Keywords:** connective tissues • crystal growth • Markov chain • polar properties • self-assembly

### Introduction

A concept for generating polar properties in systems that *grow* by a mechanism of attaching building blocks to a surface is depicted in Figure 1. By use of building blocks that possess a polar symmetry, there is a difference in the probability to attach them “tip-first” or “back-first” to the surface of a material also composed of these building blocks. As a result of a *stochastic* process of attachments (Figure 1a), a system can develop macroscopic polar properties stepwise if kinetic

stability for the grown-in orientational state of building blocks is provided (Figure 1b).

By polarity we understand here a *vectorial property* inherent to the building blocks used to assemble a material with grown-in polarity in the *bulk* state.

There are ten point groups<sup>[1]</sup> for crystals and two continuous groups<sup>[2]</sup> for non-single-crystalline materials preserving a vectorial property. The pyroelectric effect is a typical example for a polar property of crystals, poled ceramics, liquid crystals and poled polymers; a property which has found widespread technical application. A polar symmetry is basic to the function of important devices such as the diode, transistor and photovoltaic cell. With respect to morphology, most objects grown on the surface of the earth show a polar habitus: plants, animals, humans, buildings and other constructions. In biology, the polarity of cells is considered a necessary property for their regulatory function during morphogenesis.<sup>[3]</sup>

Since the middle of the last century, concepts for making materials with polar properties have been major goals in the chemistry of molecules and materials, along with the development of physical methods to characterise the macroscopically polar state (nonlinear optical, electro-optical, pyroelectric, piezoelectric effects, etc.).<sup>[4]</sup> To date, there is still no generally valid synthetic concept to assure a polar point group for crystals by a mechanism of *spontaneous nucleation*. However, crystallisation of enantiomerically pure dipolar compounds can yield one of the eleven enantiomorphic point groups, whereby ten show a piezoelectric effect. Only five (namely those featuring only a unique rotational axis: 1, 2, 3, 4, 6) of the enantiomorphic groups that are piezoelectric also allow for pyroelectricity.<sup>[1b]</sup>

Conceptually, the certain way to obtain a continuous polar group ( $\infty$ ,  $\infty m$ ) for a material is the use of an *external* electrical field to pole polymeric layers or ferroelectric ceramics during cooling through the transition temperature.

Recently, a general principle of spontaneous polarity formation by a stochastic process of growth has been stated and experimentally confirmed.<sup>[5]</sup> A vectorial property is preserved by symmetry at the nutrient-to-solid interface of whatever growing bulk material. In the case of polar building blocks, bulk polarity will result if polarity generated at the surface is kinetically stabilised during the continuation of growth (Figure 1).

---

[a] Prof. Dr. J. Hulliger  
Department of Chemistry and Biochemistry  
University of Berne  
Freiestrasse 3, 3012 Berne (Switzerland)  
Fax: (+41) 31-631-3993  
E-mail: juerg.hulliger@iac.unibe.ch

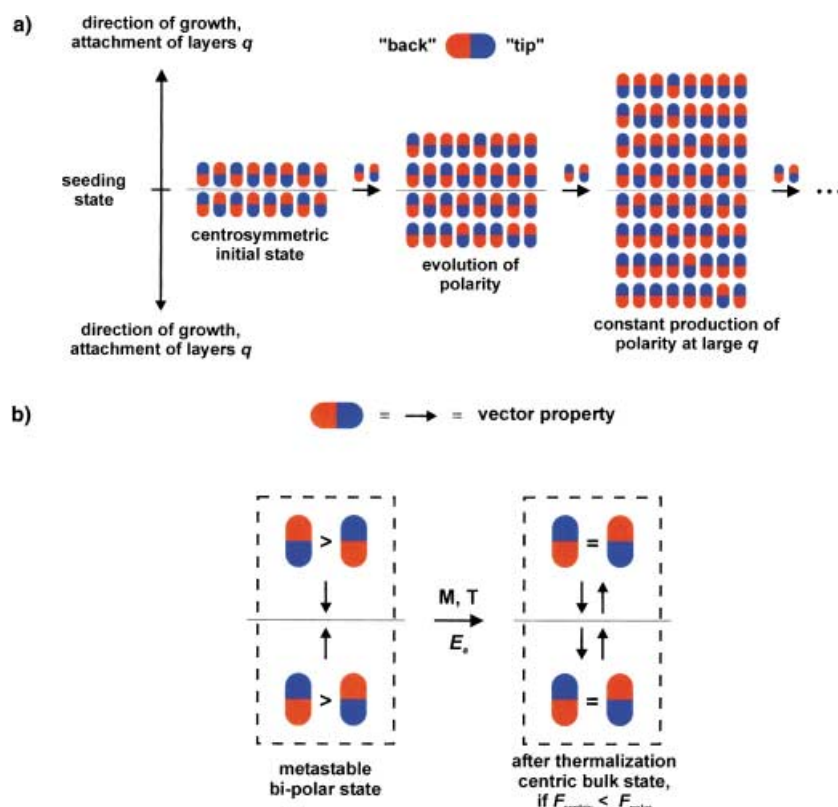


Figure 1. Graphical summary on the process of polarity formation by a mechanism of directional growth. Here, building blocks are symbolised by polar pearls attached to a surface. a) Polar building blocks are shown; these become attached to a substrate by a process of directional growth (shown on the left). Because of the perfect order of an “up” and “down” orientation in the substrate, there is no initial polarity, that is, excess of one preferred orientation of pearls. As growth starts (middle) there is the possibility of *faulted* orientations as compared to the centrosymmetric order within in the substrate. As growth proceeds (right) a constant state of polar order will establish, if  $P_{\text{tip-first}}$  differs from  $P_{\text{back-first}}$  (see also Figure 3). It is important to note that attachment is assumed to occur pearl- or layerwise. For pearls or layers of pearls that were attached previously, it is assumed that no re-orientational flips occur during further addition of building blocks. Because of growth into the upper and lower space, a bipolar (twinned) macroscopic state is obtained. b) As a result of growth without re-orientational flips of the previously attached building blocks, a metastable (bipolar) state is obtained. Mechanical (M) or thermal (T) activation ( $E_a$ ) may transform this grown-in state into a state represented by the best geometrical (mechanical) packing or free energy  $F$ . Depending on the system to be looked at, a centrosymmetric or polar (or just noncentrosymmetric, see comments in text on pyroelectric and piezoelectric symmetry groups) state may result upon activation.

Below we give examples from the *mechanical* world (randomly grown heaps of hard polar bodies), *crystal growth* (supramolecular and other compounds) and *biological growth of tissues* (tendon, bones, teeth). At first we provide an introduction to a Markov-chain model, unified to explain polarity formation in all systems to be discussed later on.

## Markov-chain Model of Polarity Formation

Markov-chains are used in chemistry, physics and other fields<sup>[6]</sup> to model processes represented by subsequent events  $E_0 \rightarrow E_1 \rightarrow E_2 \rightarrow \dots$ . A simple Markovian chain results if a transition matrix involving constant probabilities  $P$  promotes an initial vectorial state  $S_0$  stepwise into a final one  $S_q$  by Equations (1)–(4):

$$S_1 = P S_0 \quad (1)$$

$$S_2 = P S_1 \quad (2)$$

$$S_3 = P S_2 \quad (3)$$

$$S_q = P^q S_0 \quad (q = 1, 2, \dots, \infty) \quad (4)$$

Equation (4) may, for example, serve to model the opinion change<sup>[6d]</sup> of a committee on whatever subject (Figure 2). For example, if the promoters ( $Y$ ) of the debate are holding on (probability equal to 1) and the opponents ( $N$ ) are changing into  $Y$  with a probability of 0.5, it will take about six debates to have a nearly polarised collective opinion if the starting ratio  $Y/N = 50:50\%$ .

It is important to note that the first step, Equation (1), can itself yield a polar state if  $P_{\text{tip-surface}} \neq P_{\text{back-surface}}$ . Examples of this are ordered monolayers of dipolar molecules attached to a surface (Langmuir–Blgett films and others).

Applied to polarity formation as introduced above, we define here probabilities  $P$  that account for an object to object-at-surface recognition shown in Figure 3. In view of interactions of polar molecules,<sup>[4]</sup> we may denote the “back” by  $A$  and the “tip” by  $D$ . The molar fraction  $X$  of objects at a surface layer presenting their  $A$  or  $D$  part toward the nutrient is  $X_A$  or  $X_D$ , respectively, whereby  $X_A + X_D = 1$ . The net fraction  $X_{\text{net}}$  of a resulting vectorial property

(polarisation  $\mathfrak{P}_s$  proportional to  $X_{\text{net}}$ ) is defined by Equation (5).

$$X_{\text{net}} \equiv X_A - X_D \quad (5)$$

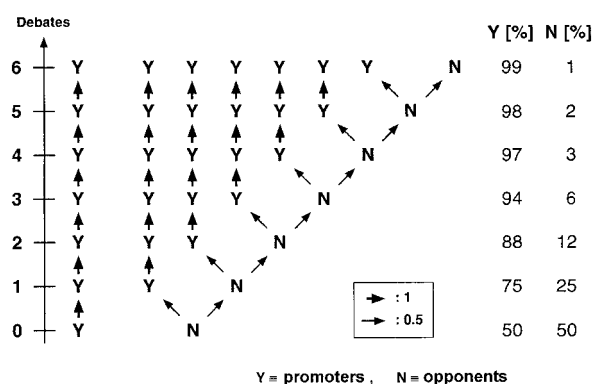


Figure 2. Illustration for an application of a Markov chain model in opinion change during repeated balloting. Starting by 50 % promoters ( $Y$ ) and 50 % opponents ( $N$ ), a polarised opinion can emerge as a result of debates. A probability of 0.5 for a conversion of  $N$  into  $Y$  was assumed.

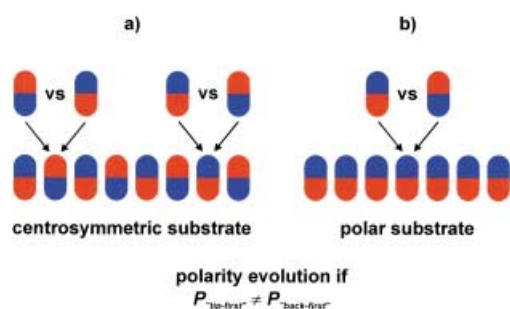


Figure 3. Polarity formation as discussed arises because of an orientational selectivity of polar building blocks undergoing attachment to a surface. a) For a *centrosymmetric* substrate there are two different attachment sites which show up by the “tip” or “back” at the surface. b) In the case of an *uniformly polarised* substrate there is only one type of site, either “tip” or “back” appearing at the surface.

The probability  $P$  to have A toward the nutrient when attached to a surface site A is called  $P_{AD}$ , because the D part of the incoming object is assumed to interact with i) the A part of a building block at the surface and ii) the surrounding blocks attached before. Correspondingly, we have  $P_{DA}$ ,  $P_{AA}$  and  $P_{DD}$ , whereby  $P_{AD} + P_{AA} = 1$  and  $P_{DA} + P_{DD} = 1$ . Equation (4) then extends with the inclusion of these probabilities to a  $2 \times 2$  matrix representation [Eq. (6)].<sup>[7, 8]</sup>

$$\begin{pmatrix} X_A(q) \\ X_D(q) \end{pmatrix} = \begin{pmatrix} P_{AD} & P_{DD} \\ P_{AA} & P_{DA} \end{pmatrix}^q \begin{pmatrix} X_A(0) \\ X_D(0) \end{pmatrix}, \quad (6)$$

in which  $X_A(0)$ ,  $X_D(0)$  describe the initial state at the surface subjected to growth ( $q = 1, 2, \dots, \infty$ ) and  $X_A(q)$ ,  $X_D(q)$  are the fractions after  $q$  steps of attachment. Equation (6) has an interesting mathematical property;<sup>[6]</sup> at large values of  $q$  the final state is independent of the initial distribution of A and D at the surface of a seeding state. Only evolution of polarity into a constant  $X_{\text{net}}$  depends on the initial state, whereas the final value of  $X_{\text{net}}$  ( $q \rightarrow \infty$ ) does not (Figure 4). It

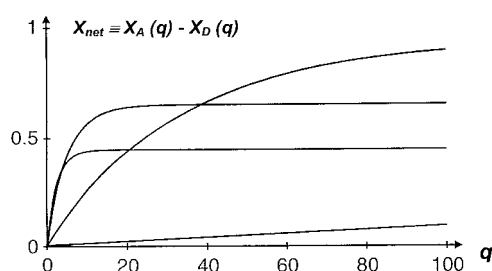


Figure 4. As defined in the text, polarity is expressed by the net fraction  $X_{\text{net}}$  [Eq. (5)] of a preferred dipolar orientation. Physically, the polarisation  $\Psi_s$  is proportional to  $X_{\text{net}}$ . The graphs show the evolution of  $X_{\text{net}}$  as a function of the growth steps ( $q$ ) in one of the two directions in space. A bipolar structure is formed (e.g., as in bones, see Figure 9), if growth can take place in both directions of a prolate-top object. A steep or a flat increase of  $X_{\text{net}}$  is possible, depending on probabilities  $P$  involved in the transition matrix in Equation (6).

is the *ergodic* property of a Markov chain which makes the present model so interesting for understanding the building up of a vectorial property, because a *centrosymmetric* initial state can undergo evolution into a *noncentrosymmetric*, more precisely, *polar* one by a process of unidirectional growth.

Asymptotic limits are given by Equations (7) and (8).

$$X_A = \frac{P_{DD}}{P_{AA} + P_{DD}} \quad (7)$$

$$X_D = \frac{P_{AA}}{P_{AA} + P_{DD}} \quad (8)$$

Evidently, polarity can evolve only if  $P_{DD} \neq P_{AA}$ . Whatever makes a “tip-to-tip” (or “tip-to-surface”) interaction different from a “back-to-back” (or “back-to-surface”) one, it is this difference which drives the system to polarity as growth proceeds, irrespective of interactions to neighbouring blocks that may tend to suppress polarity.<sup>[8]</sup> Depending on the elements of the transition matrix in Equation (6), polarity may evolve over just a few or a very large number  $q$  of steps. Graphical examples for the rise of polarity (for sets of assumed probabilities) are shown in Figure 4. In the general case interactions between incoming building blocks and the surface (longitudinal) as well as interactions between blocks within the newly attached layer (transversal) are taken into account to calculate the probabilities.<sup>[8]</sup>

## Examples from the Mechanical, the Crystalline and the Biological World

**Piling sugar beets and similar objects into heaps:** When Swiss farmers are harvesting sugar beets they pile them on their fields into huge heaps. Passing these on a walk, we may ask: Will a random process of piling polar objects into a heap create a vectorial property? The answer is yes! Laboratory experiments with beet-shaped plastic pearls have shown the formation of a vectorial-type property if the pearls are piled by a random process of unidirectional growth into one-<sup>[5a]</sup> two- and three-dimensional stacks (see Table 1). Irrespective of the type of the geometrical confinement imposed on the pearls (entering a tube, slit or cylinder; see Figure 5), pearls showed a preference to enter “tip-first” into different types of stacks. Important to notice here that gravity (for experiments with a two- or three-dimensional confinement) would promote an orientation in which the “back” preferably faces the surface. Comparison with stacks prepared by shaking the final number of pearls within the confining box (two- and three-dimensional) has demonstrated that the grown state represents a mechanically metastable arrangement (mechanical

Table 1. Experimental results on mechanical analogues.  $n$ : number of pearls,  $X_{\text{net}}$ : see also definition by Equation (5).

Dimensionality of confinement	Number of independent trials/sampling	Mean value of $-X_{\text{net}} \equiv \frac{n_{\text{tip}} - n_{\text{back}}}{n_{\text{tip}} + n_{\text{back}}}$	Standard deviation
1D	52	0.51 <sup>[a]</sup>	0.003
2D (growth)	20	0.11	0.008
2D (randomized)	15	0.001	0.006
3D (growth)	15	0.050	0.009
3D (randomized)	22	−0.001	0.008

[a] By use of histograms<sup>[5a]</sup> a different degree of polar order (1D) was reported previously with the same set of data. Note that mechanical post-growth activation (M, see Figure 1 b) cancels polarity in the case of 2D and 3D confinement. Stochastically grown heaps of mechanical objects thus develop a *metastable* state of arrangement featuring a vectorial property.



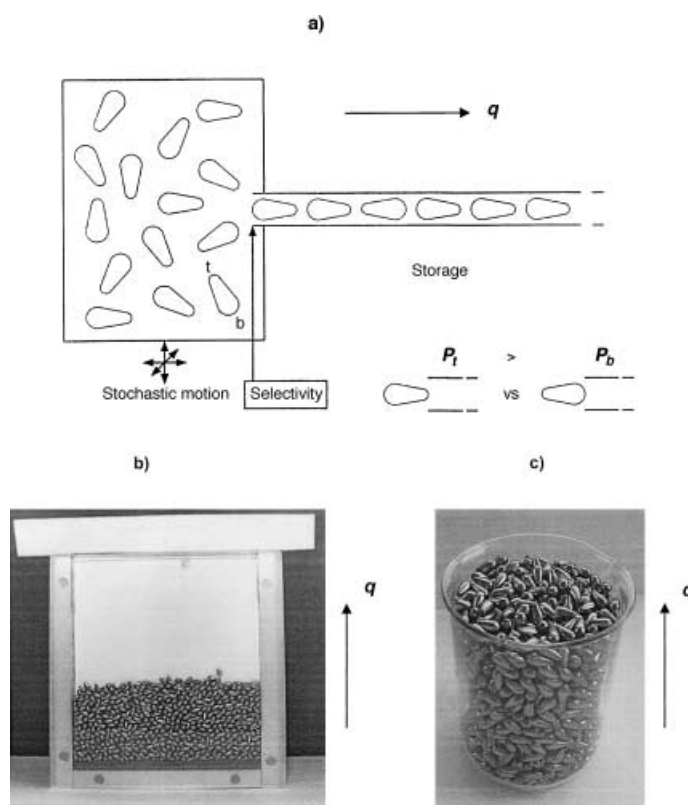


Figure 5. Mechanical confinements imposed on pearls entering a) a tube ( $l_{\text{pearl}} > d_{\text{tube}} > d_{\text{pearl}}$ ), b) a slit ( $l_{\text{pearl}} > d_{\text{slit}} > d_{\text{pearl}}$ ) and c) a cylinder ( $d_{\text{cylinder}} \gg l_{\text{pearl}}, d_{\text{pearl}}$ ), whereby  $l$  = length,  $d$  = diameter or width. Conditions for a random process of entering a containment was set up 1) by exposing pearls to a random motion in oil (a), and 2) random feeding from a high less than 10 cm above the growing layer (b, c).

(M) activation, see Figure 1b). No significant effects were found for a randomised *bulk* state (two- and three-dimensional). Given these relatively low values of  $X_{\text{net}}$  (two- and three-dimensional cases), it is likely that vectorial property formation in this particular system occurs within each full layer, thus showing little influence of the previous one. A similar situation was found for crystals in which a small number of orientational defects occur.<sup>[8a]</sup> It is anticipated that orientational disorder in some protein crystals of globular proteins may arise by a similar mechanism as demonstrated here for mechanical objects.

**Growing molecular crystals:** For the purpose of presenting a concept applying to crystalline materials we will constrain our discussion to molecules with no centre of symmetry; these do not necessarily represent chiral objects. Dipolar (achiral) compounds may be described as being composed of electron-accepting and -donating fragments symbolized by A and D, respectively. This type of a A–D molecular structure ensures polarity at the level of building blocks.<sup>[4]</sup> During the process of slow crystal growth, A–D entities enter crystal surfaces ( $hkl$ ) at which specific short-range and many long-range interactions account for the energy of attachment sites.

In crystalline materials, stochastic polarity formation was experimentally found for:

- 1 Inorganic<sup>[9]</sup> and organic<sup>[10]</sup> channel-type zeolites, whereby guest molecules enter pre-existing empty or partially filled

channels from both sides of pores by one-dimensional diffusion. In this respect, zeolites show a strong analogy to our one-dimensional mechanical analogue.

- 2 Channel-type inclusion crystals,<sup>[11]</sup> whereby guest and host molecules co-crystallise to form a supramolecular material with a centrosymmetric host structure.
- 3 Organic solid solutions  $H_{1-x}G_x$  (H: host, G: guest),<sup>[12]</sup> whereby, for example, A–D guest molecules substitute sites in a centrosymmetric lattice built by molecules H.
- 4 Single component organic crystals,<sup>[8, 13]</sup> whereby A–D molecules undergo  $180^\circ$  orientational disorder during growth, thereby transforming a centrosymmetric seed into a twinned crystal with polarity in the growth sectors.

Given whatever a type of packing and symmetry in molecular crystals (examples 1–4 above), we assume here a set of sites to which attachments can be described by probabilities  $P$  entering a kind of equation given above [Eq. (6)]. By virtue of properties of Equation (6), polarity can evolve upon a centrosymmetric seed. In such type of a seeding lattice there are at least two sites related by a centre of symmetry. During growth, corresponding sites appear at the crystal surface whereby the centre of symmetry is lost (because of joining the nutrient, i.e., interface formation). Therefore, we may approach polarity evolution by *two* independent Markov-chains,<sup>[8]</sup> for which longitudinal (A–D to surface interactions) and transversal (A–D intralayer interactions) interactions of molecules must be known for the calculation of probabilities  $P$  in Equation (6). Precisely, our system was investigated by an anisotropic two-dimensional Ising Hamiltonian that formally includes the effect of an external field.<sup>[14]</sup> The appearance of an external electrical field here shows similarity to the certain way to obtain a continuous polar group ( $\infty, \infty m$ ) by a process of electrical poling. Bethe–Peierls and Markov mean-field solutions of the Hamiltonian agree well with Monte–Carlo simulations, which take into account an attachment layer (or bilayer) of A–D molecules subjected to thermalisation on top of a frozen substrate layer of A–D molecules.<sup>[8, 14]</sup>

Because of a centric seed to start with, polarity evolution for the most frequent space group reported for molecular compounds,  $P2_1/c$ , takes place symmetrically in corresponding growth sectors, for example, the  $+b$ - and  $-b$  sector (for comparison, see Figures 1 and 6).<sup>[15]</sup> Consequently, as-grown crystals are twinned. In sectors related by the symmetry of the seeding point group, corresponding vectors of average macroscopic polarity are, in theory, of equal absolute value, but have an opposite orientation. This type of a nongeometrical twinning is typical for grow-in polarity in crystals<sup>[8]</sup> and other systems (see biological examples of bones, Figure 9 below). It is important to mention here that polarity evolution is not necessarily the result of a kinetically controlled growth process, although we have conditioned it to kinetic stability (see Figure 1b).

Experimentally,  $180^\circ$  domain formation was recently confirmed by two independent new techniques: scanning pyroelectric microscopy (SPEM)<sup>[16]</sup> and phase-sensitive second harmonic microscopy (PS-SHM).<sup>[17]</sup> These analytical methods allow the mapping of the spatially inhomogeneous distribution of polarity in crystals and thin layers. The lateral

resolution of SPEM is presently at about  $2.5\ \mu\text{m}$ ; in PS-SHM two-dimensional resolution is limited by far-field optics and the wavelength of the fundamental laser light.

The existence of polarity and  $180^\circ$  twinning in examples 1–4 has been confirmed by SPEM or PS-SHM, and X-ray diffraction (type 3).<sup>[12a,b]</sup>

Examples of type 1 (lattices providing channels) show similarity to a diffusion process of molecules across pores of natural or artificial membranes.<sup>[18]</sup> However, a most recent case of polarity inversion, found (molecular dynamics simulations) for the average dipolar moment of water passing along the pore of aquaporins (AQP1, GlpF),<sup>[19]</sup> occurs as a result of interactions to binding sites at the wall, rather than by the water-to-water interaction along the water chain seen across the pore. Another case of great importance in biology are microtubules in neuronal and other cells: microtubules in the axon of neurons show a high degree of polar order; this gates the direction of flow of material across the neuron.<sup>[20]</sup>

For a brief discussion of a most recent example<sup>[8b, 13]</sup> from the crystalline world (type 4), Figure 6 depicts 4-chloro-4'-nitro-stilbene (CNS) entering a crystal lattice in the *b* sector of

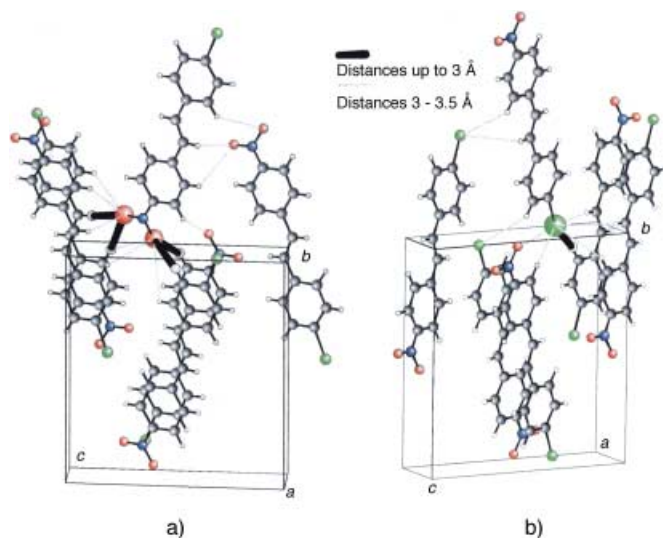


Figure 6. 4-Chloro-4'-nitro-stilbene (CNS) molecules entering the centrosymmetric lattice in a *b* sector. a) Entering by “NO<sub>2</sub>-group first” establishes four N–O...H–C bonds in the range of 2.4–2.8 Å. b) Entering by “Cl-group first” establishes only one Cl...H–C bond of 2.8 Å. For clarity, only molecules that form relatively short bonds to the NO<sub>2</sub> or Cl groups are shown here. The orientation of CNS in the unit cell is set at random because of the centrosymmetric crystal structure.<sup>[8b]</sup>

$P_{21}/c$  by a) “nitro-first” or b) “chloro-first”. In case a) there are four relatively short O...H–C bonds. In case b) there is only one relatively short Cl...H–C bond. Although we do yet not know the difference in energy that gives rise to  $P_{\text{chloro-surface}} \neq P_{\text{nitro-surface}}$ , it is reasonable to assume a small difference here. The effect of polarity formation is confirmed by a second harmonic generation (SHG) response seen in CNS crystals:<sup>[13]</sup> for the first time, a grown-in bipolar state was confirmed for  $P_{21}/c$ . In Figure 7A a fundamental-wave-polarised parallel *b* axis reveals the presence of polarity in both the upper and lower *b* sectors. The phase-sensitive response<sup>[17]</sup> has an opposite orientation for the polarisation

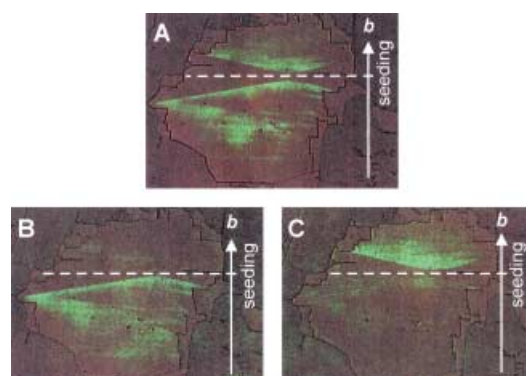


Figure 7. Second harmonic generation analysis to show polarity formation in the centrosymmetric crystal structure (X-ray analysis) of 4-chloro-4'-nitrostilbene.<sup>[8b, 13]</sup> Micrometer thin crystal plate in (001) orientation, grown from the melt. A) Polarisation of the fundamental wave (1064 nm) parallel the *b* axis (upper and lower *b* sector appearing green, 512 nm). B) Effect of phase contrast for the lower *b* sector (only SHG signals from here). C) Effect of phase contrast for the upper *b* sector. A change of contrast with respect to the lower and upper sector allows one to conclude that the orientation of the average polarisation in the lower sector (B) is opposite to that in the upper one (C). Going back to Figure 1, nonlinear optical microscopy confirms here a basic feature of Markov-type polarity formation.<sup>[8]</sup>

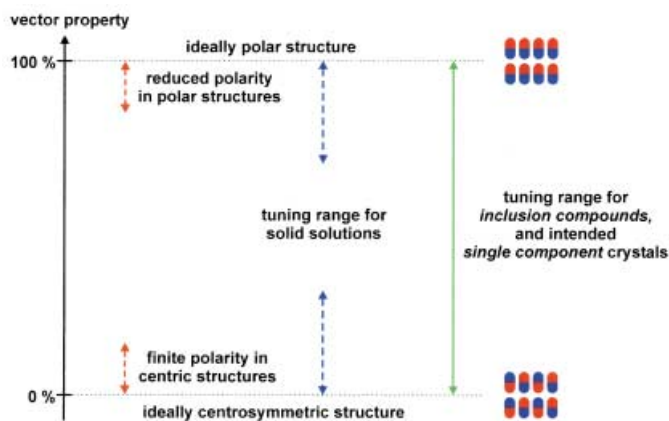


Figure 8. Summary of the possibilities for tuning polarity by use of different crystalline systems: 1) Full tuning range for channel-type inclusion compounds and intended single component crystals. 2) Limited ranges for tuning of solid solution (with respect to the range of composition). 3) Limited ranges for either topologically polar or centrosymmetric single component crystals.

vector  $\mathfrak{P}_s$  in the upper and the lower *b* sectors (Figure 7B, C). Sectors that feature an SHG response do not take up a “closest possible approach” conformation, due to seeds that grew first along the *a* axis before developing along *b* axis. Other crystals were investigated, for which this gap was not seen.<sup>[13]</sup> For geometrical reasons the SHM effect is below the present detection limit for *a* sectors in CNS.

Conceptually, we find for molecular crystals that polarity is a *tunable* (tuning variables can be: strength of synthon interactions, composition, growth temperature) property (Figure 8) that can be obtained by application of an unifying principle.<sup>[5]</sup> Broken lines in Figure 8 indicate that the extent of polarity which may be found depends on interactions active during crystal growth. In the case of solid solutions there might be a miscibility gap for a system in which A–D

molecules substitute sites in a centrosymmetric lattice of A–A or D–D molecules or vice versa. The miscibility gap is likely to exist, since examples of A–D (centrosymmetric, synthon interactions present) forming a solid solution with A–A or D–D (centrosymmetric) over the entire range of composition may represent a rare case.

**Biologically grown tissues:** By a process called morphogenesis nature creates all kind of macroscopic forms that are basic to the mechanical stability of the living world.<sup>[21]</sup> Soft, elastic and hard materials emerge from a cell-driven intergrowth of biopolymers and inorganic crystalline compounds in the case of hard tissues. Connective-tissue proteins such as collagen, elastin and others serve to hold cells together; they provide not only elastic properties but also space-filling and interfacial properties.

Collagen,<sup>[22]</sup> a family of fibrous proteins, is the most abundant protein in nature used as major fibrous component to grow tendon, bones and teeth, etc. In non-cross-linked tropocollagen three polypeptide chains form a triple helix. Each strand of the triple helix is made up mostly from the sequence gly-pro-pro; however, other amino acids occur as well. Tropocollagen can self-assemble into fibrils that are up to hundreds of micrometers long. The synthesis of an extracellular matrix that contains long collagen fibrils is prerequisite for the morphogenesis of tissues.

Because of its helical peptide structure and side-chain amino acids that introduce charged groups along the helix, tropocollagen is a *chiral* and *polar* macromolecule. In hard tissues, the structural organisation of collagen fibrils is a staggered, parallel array intergrown by inorganic crystallites.<sup>[23]</sup> Looked at as a noncrystalline but partially ordered material, the order of collagen molecules or fibrils may be described by a continuous group ( $\infty$  or  $\infty 2$ ). For comparison,<sup>[2]</sup> nematic liquid crystals made of optically active and polar molecules can exist in symmetry  $\infty$  allowing for piezoelectric, nonlinear optical (third rank tensorial properties) and pyroelectric (vectorial property) effects. In group  $\infty 2$  we find nematic liquid crystals composed of optically active molecules with third rank tensorial but no vectorial properties.

Tropocollagen has the potential to act as a building block to form either a material with  $\infty$  or  $\infty 2$  symmetry. Given a case of *parallel* alignment of helices (type I packing of collagen fibrils, see Weiner<sup>[24]</sup> et al.), corresponding tissues will show a *transversal* piezoelectric and second-order nonlinear optical effect ( $\infty 2$ ). In the Introduction we noted that a chiral molecular structure can ensure formation of a crystal lattice belonging to one of the enantiomorphic groups. However, there is no guarantee that they will fall into a pyroelectric group as well.

To obtain polar symmetry ( $\infty$ ) when building a collagen-based composite material, a mechanism is needed which drives the ordering of collagen along the process of secretion and self-assembly into a vectorial alignment in mature fibrils. Biological studies show that fibril self-assembly takes place in extracytoplasmic channels of fibroblasts (for more details, see ref. [25]).

Since the second half of the last century it is known that biologically grown soft and hard tissues show effects related to

electrical polarity.<sup>[26]</sup> First it was found that bones have a transversal piezoelectric effect ( $\infty 2$ ).<sup>[27]</sup> Later, evidence for small *longitudinal* piezoelectric<sup>[28]</sup> (Fukada et al., 1964) and *pyroelectric* effects<sup>[29]</sup> was reported. Although hard tissues contain hydroxyapatite,  $\text{Ca}_5(\text{PO}_4)_3(\text{OH})$ , effects of polarity cannot have their origin in a textured ( $\infty$ ,  $\infty m$ ) mineral intercalation, as centrosymmetric space groups are found for modifications of hydroxyapatite ( $P6_3/m$  or  $P2_1/b$ ).

Athenstaedt<sup>[30]</sup> has extensively studied the pyroelectric properties of many kinds of hard tissues and tendon. According to Athenstaedt pyroelectric effects exist in “nerve tissue, in the integument of vertebrates and arthropods, in all major supporting tissues of the vertebrates and [...] in cells and tissues of plants”.<sup>[31a]</sup> Taking into account its broad appearance it seems that pyroelectricity (and logically a longitudinal piezoelectric effect) is a basic property of all living organisms. There is another general finding: the unidirectional growth of animal (tendons, bones, teeth) and plant structures occur always in the direction of the positive pole (for a definition, see Figure 9), irrespective of whether

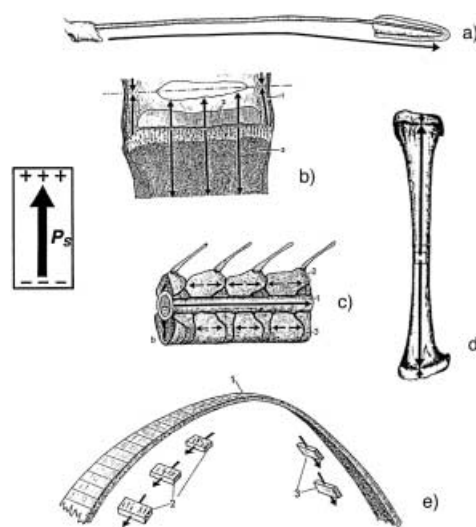


Figure 9. Some examples of bones with either an unipolar or a bipolar state as a result of biological growth (H. Athenstaedt<sup>[30, 31]</sup>). Arrows (drawn into bones) represent parts of an uniform orientation of polarisation  $\mathfrak{P}_s$  ( $P_s$  in the figure here). Along the arrows collagen fibrils show a preferred vectorial alignment (excess of one orientation of a few percent<sup>[32, 34]</sup>). Note that the positive pole points in the direction of longitudinal biological growth. The Markov chain model that makes use of biochemical results<sup>[35, 36]</sup> to obtain an order of probabilities  $P$  agrees with experimental findings on the orientation of net polarity.<sup>[30, 31]</sup> a) Exposed chorda of *Myxine glutinosa*; b) part of the axial skeleton of *Acipenser sturio*; c) *Macropus spec.* (Marsupialia), young animal during growth of axial skeleton; d) parietal bone of a new-born child (at the parietal tuber 1 the direction of polarisation is reversed), e) fibula of *Crocodilus niloticus*.

collagen-, keratin-, chitin-based materials were investigated. When comparing hard tissues with tendon, effects in collagen-rich tissues are larger by about a factor of ten. After the period of growth, aging can reduce or even invert the grown-in polarisation. This not true for collagen-rich structures of the axial skeleton (disci intervertebrales, ligamenta longitudinalia communia<sup>[30, 31b]</sup>). Our discussion will therefore be restricted to polarity evolution in young, growing tissues.

Independent work with second harmonic generation techniques including second harmonic microscopy<sup>[32]</sup> (also tomographic, confocal and ultrashort pulse studies<sup>[33]</sup>) has confirmed the  $\infty 2$  symmetry and particularly supports polarity formation in tendon ( $\infty$ ). Freund et al.<sup>[32]</sup> could show that most, if not all, polar filaments are of the same sign, and that these filaments permeate the tendon bulk in an apparently random fashion. Furthermore, they have estimated that the polar material occupies a few percent of the tendon volume. An electron microscopy study by Trelstad et al.<sup>[34]</sup> reports a 53% fraction of the collagen molecules in tendon oriented in the same direction. Both kind of data allow for a small excess of fibrils oriented in the same direction.

A recent study by Kadler et al.<sup>[35]</sup> has identified two types of fibrils in 12- and 18-day-old embryonic (chick metatarsal leg) tendon that differ with respect to the orientation of collagen molecules in the fibrils: 1) unipolar fibrils joined by the C and N termini, and 2) bipolar fibrils joined by the C termini. The mean length of unipolar fibrils is found to be smaller than for bipolar ones (bipolar/unipolar fibrils = 2:1). Growth into long unipolar and bipolar fibrils seems to be supported by proteoglycans, which are preferably attached to the shafts of the fibrils, leaving more space at the tips for a process of longitudinal self-assembly.

In view of our Markov chain model, polarity formation in longitudinally growing tendon may be analysed in the following way: at first we define the building blocks subjected to self-assembly. Next, interactions are identified by which these blocks can self-assemble in the longitudinal direction. Finally a model for unidirectional growth is proposed.

Referring to a review by Kadler et al.,<sup>[36]</sup> fusion of fibrils has been observed to occur 1) by interaction of the C and N

termini (producing unipolar fibrils of an increased length), and 2) by interaction of the C termini (producing a bipolar fibril from two unipolar ones). Fusion by interactions of N-termini was not reported. Given these results, we define short unipolar fibril segments to act as building blocks to obtain finally a macroscopic object of tendon. As a matter of fact, the probabilities  $P_{CN}$ ,  $P_{NC}$  (prolongation) and  $P_{CC}$  (bipolar fusion) are significant, whereas  $P_{NN}$  (fusion by N termini) is negligible. From the chemical point of view it is thus reasonable to assume  $P_{CN} \gg P_{CC}$ . (Note that  $P_{CN} + P_{CC} = 1$ ,  $P_{NC} + P_{NN} = 1$ .) At this point we can say that  $P_{CC} \neq P_{NN}$ , which is the necessary condition for polarity formation.

Polarity evolution at the level of the early state of a piece of tendon may start with an equal number of “up” and “down” fibrils exceeding elongation in extracytoplasmic channels (Figure 10). In this sense we model the system by two independent Markov chains (I, II, see Figure 10), an approach we have discussed in the chapter on crystals.<sup>[8]</sup> Driving forces for lateral aggregation may support or work against polarity formation.<sup>[8]</sup> As a result of the interplay of all interactions, in principle, polarity will develop if the difference in  $P_{CC}$  and  $P_{NN}$  is effected by a stochastic mechanism of self-assembly. Because  $P_{CC} > P_{NN}$ , the positive ends (N termini) of the fibrils will preferably point in the direction of growth (see Figure 10). This important prediction of the Markov chain model agrees with experimental data.<sup>[30, 31]</sup> A similar mechanism is proposed for bones and teeth, although hard tissues exceed intercalation by apatite in the late phase of development.

In view of a broad occurrence of polarity in tissues, the biological function of a  $\infty$ -type symmetry should be questioned. Is it just a stochastic phenomenon, for example, some

kind of a defect, or is there a functionality behind it? Investigations in the field of bioelectrical potentials<sup>[37]</sup> have forwarded the possibility of an electrical-signal-feedback sensor system because of electrical polarity in connective tissues. Basic principles for sensory functions and organs using polar dielectric properties were proposed by Athenstaedt.<sup>[38]</sup> Examples of sensory properties are the piezoelectric auditory membrane of the ear of *locusta migratoria* (insect)<sup>[38]</sup> and the infrared-sensitive organ of *Crotalinae* and *Boidae* (snakes).<sup>[39]</sup> Today, biologists are investigating a possible sensory function of thermophilic proteins (vanilloid-like receptors: VR1, VRL),<sup>[40]</sup> although a pyroelectric behaviour of the membrane of *Crotalus horridus* (rattlesnake) was demonstrated much earlier.<sup>[41]</sup>

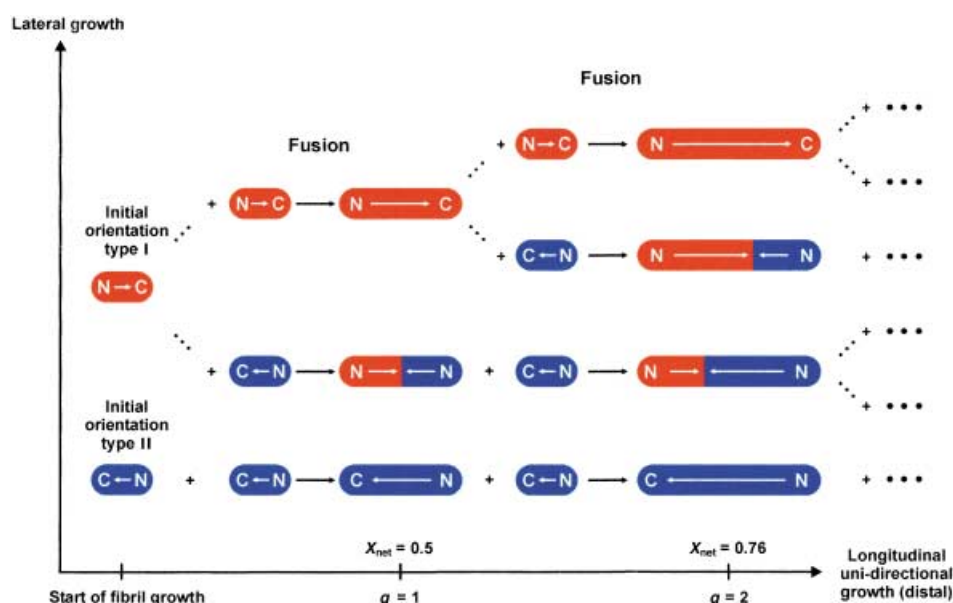


Figure 10. Graphical scheme for explaining polarity formation in tissues grown by self-assembly of small unipolar fibril segments.  $q$ : subsequent steps of fusion. The length of arrows is a measure for the polarity of fibrils. For a demonstration  $P_{CN} = P_{CC} = 0.5$  was chosen. In this case polarity evolves already after the first step ( $q = 1$ ). Biochemical data<sup>[35, 36]</sup> on the early state of tendon development imply, however, that  $P_{CN} \gg P_{CC}$  and  $P_{CC} > P_{NN}$ . Therefore, a much larger number of growth steps than  $q = 1, 2$  are needed to produce a significant  $X_{net}$  of a few percent as found experimentally.<sup>[32, 34]</sup> For more theoretical details on Markov-type polarity formation, see Hulliger et al.<sup>[8]</sup>



## Conclusion

We present an unifying concept of how a process of unidirectional growth can build up macroscopic polarity in materials. It turns out that polarity at the level of building blocks (mechanical, molecular, supramolecular, macromolecular) is the key for preserving polarity along a *stochastic* process of self-assembly. As compared to cooperative phase transitions generating polarity in the bulk, a growth-driven transition into a metastable polar state is generally not subjected to the option of a centre of symmetry. However, if growth is allowed in the + and – direction of space, bipolar objects evolve. In this sense the Markov chain mechanism produces macroscopic domains featuring opposite polarity. Because in nature and in vitro we can establish conditions for unidirectional growth, the present concept allows for a rational synthesis of unipolar materials.

More than 35 years after the discovery of the wide-spread existence of pyroelectricity in the living world we can put forward an explanation for polarity formation by a growth mechanism effected by chemical recognition.<sup>[42]</sup>

## Acknowledgement

This work has received support from the NFP47 “Functional Supramolecular Materials” (no. 4047-057476/1). I thank Dr. R. Fallahpour for searching the literature, Dr. S. Kluge for SHG experiments, B. Trusch and Dr. I. Dohnke for their technical assistance, Dr. Dr. H. Athenstaedt for the use of figures and stimulating discussions, and colleagues around the world for helpful advice.

- [1] a) J. F. Nye, *Physical Properties of Crystals (their Representations by Tensors and Matrices)*, Clarendon, Oxford, **1992**; b) W. Kleber, H. J. Bartsch, J. Bohm, I. Kleber, *Einführung in die Kristallographie*, 17th ed., Verlag Technik, Berlin, **1990**.
- [2] “Piezoelectric Textures”: A. V. Shubnikov, *Izv. Akad. Nauk SSSR*, **1946**.
- [3] R. L. Trelstad, *Dev. Biol.* **1977**, *59*, 153–163.
- [4] H. S. Nalwa, S. Miyata, *Nonlinear Optics of Organic Molecules and Polymers*, CRC, London, **1997**.
- [5] a) J. Hulliger, *Z. Kristallogr.* **1999**, *214*, 9–13; b) “Crystal Engineering: From Molecules and Crystals to Materials”: J. Hulliger, S. W. Roth, A. Quintel, *NATO ASI Ser. Ser. C* **1999**, *538*, 349–368.
- [6] a) C. W. Gardiner, *Handbook of Stochastic Methods (for Physics, Chemistry and the Natural Sciences)*, Springer, Berlin, **1997**; b) J. G. Kemeny, J. L. Snell, *Finite Markov Chains*, van Nostrand, London, **1983**; c) M. Iosifescu, *Finite Markov Processes and their Applications*, Wiley, New York, **1980**; d) *Readings in Mathematical Social Science* (Eds.: P. F. Lazarsfeld, N. W. Harry), MIT Press, London, **1966**.
- [7] a) J. Hulliger, P. Rogin, A. Quintel, P. Rechsteiner, O. König, M. Wübbenhorst, *Adv. Mater.* **1997**, *9*, 677–680; b) K. D. M. Harris, P. E. Jupp, *Proc. R. Soc. London Ser. A* **1997**, *453*, 333–352; c) K. D. M. Harris, P. E. Jupp, *Chem. Phys.* **1997**, *274*, 525–534; d) S. W. Roth, P. J. Langley, A. Quintel, M. Wübbenhorst, P. Rechsteiner, P. Rogin, O. König, J. Hulliger, *Adv. Mater.* **1998**, *10*, 1543–1546.
- [8] a) J. Hulliger, M. Alaga-Bogdanovic, H. Bebie, *J. Phys. Chem. B* **2001**, *105*, 8504–8512; b) J. Hulliger, H. Bebie, S. Kluge, A. Quintel, *Chem. Mater.* **2002**, *14*, 1523–1529.
- [9] a) J. Caro, F. Marlow, M. Wübbenhorst, *Adv. Mater.* **1994**, *6*, 413–416; b) F. Marlow, M. Wübbenhorst, J. Caro, *J. Phys. Chem.* **1994**, *98*, 12315–12319.
- [10] T. Hertzsch, S. Kluge, E. Weber, F. Budde, J. Hulliger, *Adv. Mater.* **2001**, *13*, 1864–1867.
- [11] a) V. Ramamurthy, D. F. Eaton, *Chem. Mater.* **1994**, *6*, 1128–1136; b) J. Hulliger, O. König, R. Hoss, *Adv. Mater.* **1995**, *7*, 719–721; c) R. Hoss, O. König, V. Kramer-Hoss, U. Berger, P. Rogin, J. Hulliger, *Angew. Chem.* **1996**, *108*, 1774–1776; *Angew. Chem. Int. Ed. Engl.* **1996**, *35*, 1664–1666; d) T. Müller, J. Hulliger, W. Seichter, E. Weber, T. Weber, M. Wübbenhorst, *Chem. Eur. J.* **2000**, *6*, 54–61.
- [12] a) M. Vaida, L. J. W. Shimon, Y. Weisinger-Lewin, F. Frolow; M. Lahav, L. Leiserowitz, R. K. McMullin, *Science* **1988**, *241*, 1475–1479; b) Y. Weisinger-Lewin, F. Frolow, R. K. McMullin; T. F. Koetzle, M. Lahav, L. Leiserowitz, *J. Am. Chem. Soc.* **1989**, *111*, 1035–1040; c) S. Kluge, I. Dohnke, F. Budde, J. Hulliger, unpublished results.
- [13] S. Kluge, F. Budde, J. Hulliger, *Appl. Phys. Lett.*, **2002**, *81*, 247–249.
- [14] H. Bebie, J. Hulliger, M. Alaga-Bogdanovic, *Phys. Rev. E* **2002**, *66*, 021605.
- [15] J. Hulliger, *Z. Kristallogr.* **1998**, *213*, 441–444.
- [16] a) A. Quintel, J. Hulliger, M. Wübbenhorst, *J. Phys. Chem. B* **1998**, *102*, 4277–4283; b) A. Quintel, S. W. Roth, J. Hulliger, M. Wübbenhorst, *Mol. Cryst. Liq. Cryst.* **2000**, *338*, 243–256.
- [17] P. Rechsteiner, J. Hulliger, M. Flörsheimer, *Chem. Mater.* **2000**, *12*, 3296–3300.
- [18] D. T. Bong, T. D. Clark, J. R. Granja, M. R. Ghadiri, *Angew. Chem.* **2001**, *113*, 1016–1041; *Angew. Chem. Int. Ed. Engl.* **2001**, *40*, 988–1011.
- [19] B. L. de Groot, H. Grubmüller, *Science* **2001**, *294*, 2353–2357.
- [20] R. Brandt, *Cell Tissue Res.* **1998**, *292*, 181–189; P. W. Baas, J. S. Deitch, M. M. Black, G. A. Banker, *Proc. Natl. Acad. Sci.* **1988**, *85*, 8335–8339.
- [21] a) S. Mann, *Angew. Chem.* **2000**, *112*, 3532–3548; *Angew. Chem. Int. Ed. Engl.* **2000**, *39*, 3392–3406; b) S. Mann, *Biomaterialization (Principles and Concepts in Bioinorganic Materials Chemistry)*, Oxford University Press, Oxford, **2001**.
- [22] D. J. Prockop, K. I. Kivirikko, *Ann. Rev. Biochem.* **1995**, *64*, 403–433.
- [23] U. Plate, S. Arnold, U. Stratmann, H. P. Wiesmann, H. J. Höhling, *Connect. Tissue Res.* **1998**, *38*, 149–157.
- [24] S. Weiner, H. D. Wagner, *Annu. Rev. Mater. Sci.* **1998**, *28*, 271–298.
- [25] R. Trelstad, K. Hayashi, *Dev. Biol.* **1979**, *71*, 228–242.
- [26] F. A. Duck, *Physical Properties of Tissue (a Comprehensive Reference Book)*, Academic Press, London, **1990**.
- [27] E. Fukada, I. Yasuda, *J. Phys. Soc. Jpn.* **1957**, *12*, 1158–1162.
- [28] a) E. Fukada, *Biorheology* **1968**, *5*, 199–208; b) E. Fukada, I. Yasuda, *Jpn. J. Appl. Phys.* **1964**, *3*, 117–121.
- [29] S. B. Lang, *Nature* **1966**, *212*, 704–705.
- [30] a) H. Athenstaedt, *Z. Zellforsch.* **1968**, *91*, 135–152; b) H. Athenstaedt, *Z. Zellforsch.* **1968**, *92*, 428–446; c) H. Athenstaedt, *Z. Zellforsch.* **1969**, *93*, 484–504; d) H. Athenstaedt, *Z. Zellforsch.* **1969**, *97*, 537–548.
- [31] a) H. Athenstaedt, *Ann. N. Y. Acad. Sci.* **1974**, *238*, 68–94; b) H. Athenstaedt, *Ferroelectrics* **1987**, *73*, 455–466; c) H. Athenstaedt, *Arch. Oral Biol.* **1971**, *16*, 495–501; d) H. Athenstaedt, *Nature* **1970**, *228*, 830–834.
- [32] I. Freund, M. Deutsch, A. Sprecher, *Biophys. J.* **1986**, *50*, 693–712.
- [33] a) Y. Guo, P. P. Ho, H. Savage, D. Harris, P. Sacks, S. Schantz, F. Liu, N. Zhadin, R. R. Alfano, *Opt. Lett.* **1997**, *22*, 1323–1325; b) B. M. Kim, P. Stoller, K. Reiser, J. Eichler, M. Yan, A. Rubenchik, L. da Silva, *Proc. SPIE* **2000**, *3927*, 207–212; c) B.-M. Kim, J. Eichler, L. B. da Silva, *Appl. Opt.* **1999**, *38*, 7145–7150.
- [34] R. L. Trelstad, D. E. Birk, in *The Role of Extracellular Matrix in Development* (Ed.: R. L. Trelstad), Liss, New York, **1984**, pp. 513–543.
- [35] H. K. Graham, D. F. Holmes, R. B. Watson, K. E. Kadler, *J. Mol. Biol.* **2000**, *295*, 891–902.
- [36] K. E. Kadler, D. F. Holmes, J. A. Trotter, J. A. Chapman, *Biochem. J.* **1996**, *316*, 1–11.
- [37] a) J. J. Konikoff, *Ann. Clin. Lab. Sci.* **1975**, *5*, 330–337; b) A. J. Grodzinsky, *Crit. Rev. Biomed. Eng.* **1983**, *9*, 133–199; d) H. Athenstaedt, H. Claussen, D. Schaper, *Science* **1982**, *216*, 1018–1020; e) G. Regling, *Electro- Magnetobiol.* **2000**, *19*, 149–161.
- [38] H. Athenstaedt, *Jpn. J. Appl. Phys.* **1985**, *24*, (suppl. 24–2) 103–106.
- [39] E. A. Newman, P. H. Hartline, *Sci. Am.* **1982**, *246*, 98–107.
- [40] M. J. Caterina, M. A. Schumacher, M. Tominaga, T. A. Rosen, J. D. Levine, D. Julius, *Nature*, **1997**, *389*, 816–824.
- [41] “Spontaneous Polarization in Organisms”: H. Athenstaedt, Society of Molecular-Physiology and Biotechnology (Institute of Molecular-Physical Physiology), Hannover, **1986**, printed report.
- [42] J. Hulliger, unpublished results.